Hyperfine Structure of Helium-3 in the Metastable Triplet State*†

GABRIEL WEINREICH,‡ *Columbia University, New York, New York*

AND

VERNON W. HUGHES, *University of Pennsylvania, Philadelphia, Pennsylvania*

(Received April 28, 1954)

The He^3 atom in the $^3S_1$ metastable state represents a system simple enough to be calculable by modern computing methods. For this reason a measurement of the hyperfine splitting of this state is of particular interest, since it is expected that a comparison with theory will reveal some effects of relativity, quantum electrodynamics, and nuclear structure.

The measurement reported here was made by the atomic-beam magnetic resonance method. Three cubic centimeters NTP of He^3 gas was continuously circulated and purified in a closed vacuum system. Frequencies of transitions between hyperfine levels were measured in a magnetic field of about $\frac{2}{3}$ gauss, with the final precision limited by inhomogeneity of the magnetic field. The value thus obtained for the (inverted) hfs splitting is 6739.71 ± 0.05 Mc/sec.

The best theoretical value currently available is 6735.9 ± 4.7 Mc/sec, as calculated by Teutsch and Hughes from the six-term Hylleraas function (see following paper). A more informative comparison with theory awaits the calculation of a more accurate electronic wave function.

1. INTRODUCTION

THE present experiment was prompted by the extraordinary fruitfulness of measurements of the hyperfine splitting of the hydrogen isotopes.[1–3] The effects of major significance shown up by those experiment were:

(a) Relativistic effects, of order $(\alpha Z)^2$; these are predicted by the Dirac equation.[4]

(b) Quantum-electrodynamic effects. These include a correction of order α to the magnetic moment of the electron[5] and corrections of order α^2 from polarization and fluctuation energy effects.[6,7] There are also relativistic reduced-mass effects of order $\alpha m/M$ involving photon exchanges between electron and proton.[8]

(c) Effects relating to the finite size of the nucleus and the consequent error of considering it a point dipole.[8–10] The estimated[11] magnitude of the effect of possible proton structure on the hfs of hydrogen is about a part in 10^5. Whereas the experimental determination[3] is considerably better than that, present knowledge of the fundamental physical constants does not allow the calculation of the hydrogen hfs to an accuracy better than a part in 10^5. In deuterium, on the other hand, the nuclear structure effect is of relative order 10^{-4} and has been definitely observed.[3]

Similar effects are to be expected in the case of helium. The relativistic effects have been calculated,[12] and the quantum-electrodynamic effects are expected to be the same as in hydrogen.[7] Thus the nuclear structure effect, which has been estimated[13,14] to be more than a part in 10^4, is directly determined by a measurement of the hfs splitting.

Sessler[12] has calculated this effect in detail and has given numerical values for various assumed nuclear wave functions. These values vary by about 25 percent, depending on the nuclear wave function used. An experimental hfs measurement good to a part in 10^5 would give the nuclear structure effect to about 5 percent and would thus distinguish strongly between the various models of the He^3 nucleus.

The ability to produce and detect a beam of helium atoms in the $^3S_1$ metastable state[15] suggested the measurement of the hyperfine splitting of the He^3 atom in this state by the atomic-beam magnetic resonance method. Such a measurement, to an accuracy somewhat better than 1 part in 10^5, will be described in this paper. The only previous determination was an optical one[16] which yielded the result 0.221 ± 0.005 cm^{-1}, or $\Delta\nu = 6630\pm150$ Mc/sec.

The apparatus adapted for this experiment was that used for measurements of the electronic magnetic moment of the metastable triplet state of helium-4,

* Submitted by Gabriel Weinreich in partial fulfillment of the requirements for the degree of Doctor of Philosophy in the Faculty of Pure Science, Columbia University.

† Research supported in part by the Office of Naval Research.

‡ U. S. Atomic Energy Commission Predoctoral Fellow, 1951–1952; now at Bell Telephone Laboratories, Murray Hill, New Jersey.

[1] J. E. Nafe and E. B. Nelson, Phys. Rev. **73**, 718 (1948); Nagel, Julian, and Zacharias, Phys. Rev. **72**, 971 (1947).
[2] E. B. Nelson and J. E. Nafe, Phys. Rev. **75**, 1194 (1949).
[3] A. G. Prodell and P. Kusch, Phys. Rev. **88**, 184 (1952).
[4] G. Breit, Phys. Rev. **35**, 1447 (1930).
[5] J. Schwinger, Phys. Rev. **73**, 416 (1948).
[6] R. Karplus and A. Klein, Phys. Rev. **85**, 972 (1952).
[7] N. M. Kroll and F. Pollock, Phys. Rev. **86**, 876 (1952).
[8] E. E. Salpeter and W. A. Newcomb, Phys. Rev. **87**, 150 (1952).
[9] A. Bohr, Phys. Rev. **73**, 1109 (1948); F. Low, Phys. Rev. **77**, 361 (1950); F. Low and E. E. Salpeter, Phys. Rev. **83**, 478 (1951).
[10] E. N. Adams II, Phys. Rev. **81**, 1 (1951).
[11] H. A. Bethe and C. Longmire, Phys. Rev. **75**, 306 (1949).
[12] A. M. Sessler, Ph.D. dissertation, Columbia, 1953 (unpublished).
[13] V. Hughes and G. Weinreich, Phys. Rev. **91**, 196 (1953).
[14] A. M. Sessler and H. M. Foley, Phys. Rev. **91**, 444 (1953).
[15] Hughes, Tucker, Rhoderick, and Weinreich, Phys. Rev. **91**, 828 (1953).
[16] Fred, Tomkins, Brody, and Hamermesh, Phys. Rev. **82**, 406 (1951).

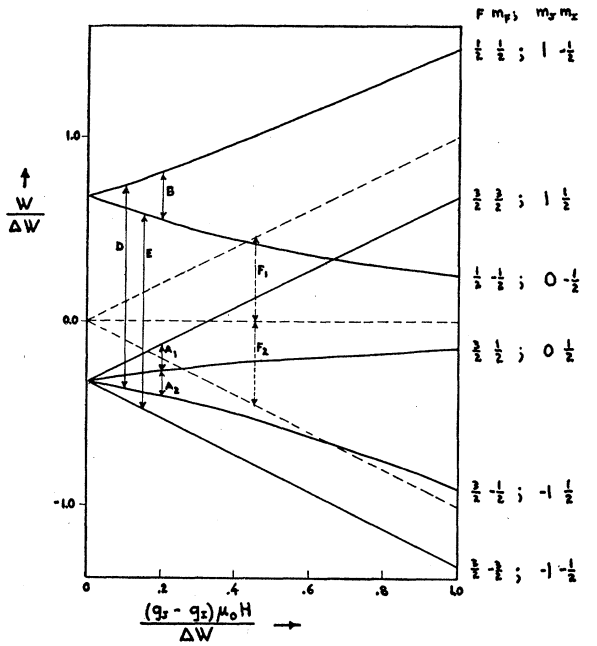

FIG. 1. Sublevels of the $^3S_1$ state in a magnetic field for He^3 and He^4.

and reference is made to the report of that experiment[15] for a description of the vacuum system, magnets, discharge tube beam source, detector, and other major features of the machine. The dimensions of the slits, magnets, and beam have not been changed. Additions to and modifications of the apparatus peculiar to the present experiment, notably a circulation system for continual re-use of the gas and a radio-frequency system for the region of 7000 Mc/sec, are described in later sections of this paper.

Unlike the case of hydrogen, the electronic wave function for helium is not known exactly, and such approximate forms as have been published in the past are much too rough to allow an adequate comparison of the present experiment with theory (see Sec. 7.5). However, it appears that the calculation of such a wave function to the required accuracy is within the possibility of present-day computing techniques.[17]

A preliminary report of the present experiment has been made.[18]

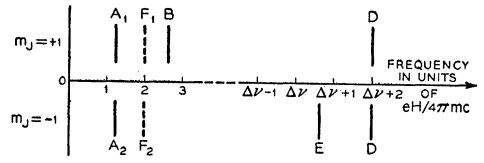

FIG. 2. Low-field transition frequencies in Lorentz units for He^3 and He^4, classified by initial m_J state.

[17] Meyerott, Luke, Clendenin, and Geltman, Phys. Rev. **85**, 393 (1952); Luke, Meyerott, and Clendenin, Phys. Rev. **85**, 401 (1952); L. H. Thomas (private communication).

[18] Weinreich, Grosof, and Hughes, Phys. Rev. **91**, 195 (1953).

2. DESIGN OF THE EXPERIMENT

2.1 Structure of the $^3S_1$ State

The Hamiltonian for the hyperfine energy levels of an atom in a magnetic field is

$$\mathcal{H}=g_J\mu_0\mathbf{J}\cdot\mathbf{H}+g_I\mu_0\mathbf{I}\cdot\mathbf{H}+a\mathbf{I}\cdot\mathbf{J},$$

where $\mathbf{J}\hbar$ and $\mathbf{I}\hbar$ are, respectively, the electronic and nuclear angular momenta, g_J and g_I the corresponding gyromagnetic ratios, μ_0 the Bohr magneton, $\mathbf{H}$ the magnetic field, and a the hyperfine interaction constant.

For the metastable triplet state of helium, J is 1. In the case of helium-4, I is zero and there is no hfs. For helium-3, I has the value $\frac{1}{2}$, and thus at zero magnetic field the level becomes a doublet of energy separation $\Delta W=h\Delta\nu=\frac{3}{2}a$.

The solid lines of Fig. 1 show the further splitting which this level undergoes when subjected to an external magnetic field. Note that, in accordance with the optical data[16] which the present experiment further verified, the hfs is shown as inverted.

The dotted lines of Fig. 1 show the linear Zeeman effect of the corresponding state of helium-4.

Explicit solutions for the energies of the six He^3 sublevels and three He^4 sublevels are listed in Table I.

2.2 Observable Transitions

For an accurate measurement of hyperfine structure it is advantageous to measure transitions at low magnetic field, for then the major part of the energy splitting is due to the hyperfine interaction rather than to the interaction with the external field. The low-field selection rules for induced magnetic dipole transitions are

$$\Delta F=0,\pm1,\quad \Delta m_F=0,\pm1,$$

where $\mathbf{F}=\mathbf{I}+\mathbf{J}$, and m_F is the corresponding magnetic quantum number.

These selection rules allow ten transitions between the six levels. Of the ten, three are unobservable in our apparatus because the associated moment changes in the high A and B fields are too small to cause appreciable defocusing of the beam. Of the remaining seven, two are so-called σ lines, i.e., transitions with $\Delta m_F=0$. These require for their excitation an rf magnetic field parallel to the static field.

It will be seen from the description of the apparatus transition region, given in Sec. 5.1, that σ lines were not observable. Thus we were left with five observable transitions.

Figure 2 indicates these five lines, with low-field frequencies in units of $eH/4\pi mc$ (Lorentz units). Explicit solutions for arbitrary values of field are listed in Table II.

A wire stop was placed in the apparatus (Sec. 5.1) so as to pass either only the $m_J=+1$ or only the $m_J=-1$ atoms selected by the A field. The transitions in Fig. 2 are therefore also classified according to

which initial m_J state is involved. It is seen that for $m_J=+1$ there are two low-frequency transitions and one high-frequency transition, and for $m_J=-1$ there are one low-frequency transition and two high-frequency transitions.

If the hfs were not inverted, the roles of the two m_J states would be reversed; thus not only the magnitude but also the sign of $\Delta\nu$ is determined by the present experiment.

The dotted lines denoted by F_1 and F_2 are the two helium-4 transitions. They were, in fact, observable in our beam since the gas sample used contained about 30 percent helium-4.

2.3 Expected Line Shapes

The usual "natural" line shape for an atomic beam experiment is derived on the assumption that an atom sees the rf field as being suddenly applied and suddenly removed.[19] In our case, however, the atom experiences the rf field by traveling through a resonant cavity; and since the cavity is in its fundamental mode, the amplitude of the rf appears to the atom modulated by a factor $\sin(\pi t/\tau)$, where τ is the transit time through the cavity. Although the "natural" line width will remain of the order of $1/\tau$, an apparatus of sufficient resolving power would reveal a shape somewhat different[20] from that of reference 19.

Such resolving power was not, however, available in our experiment because of magnetic field inhomogeneity. From previous experience with the apparatus,[21] an inhomogeneity at low fields of about $\frac{1}{3}$ gauss was known to exist; using the last column of Table II, we see that this implies widths of about 900 kc/sec and 300 kc/sec for the D and E lines, respectively. The frequency $1/\tau$, on the other hand, when one uses 10^5 cm/sec as a typical velocity and 2.24 cm as the length of the cavity (Sec. 5.1), turns out to be only about 40 kc/sec. Thus the shape of the observed line will be that determined by the inhomogeneity pattern.

TABLE I. Energies of the sublevels of a $^3S_1$ state with $I=\frac{1}{2}$ (He^3) and $I=0$ (He^4) as a function of magnetic field. Energies W are given in units of ΔW, the (inverted) hyperfine splitting at zero field; $x=(g_J-g_I)\mu_0 H/\Delta W$, $y=g_I\mu_0 H/\Delta W$.

I	F, m_F	m_J, m_I	$W/\Delta W$
$\frac{1}{2}$	$\frac{3}{2}, \frac{3}{2}$	$1, \frac{1}{2}$	$-\frac{1}{3}(1-3x)+\frac{3}{2}y$
	$\frac{3}{2}, \frac{1}{2}$	$0, \frac{1}{2}$	$\frac{1}{6}(1+3x)-\frac{1}{6}[(1+3x)^2+8]^{\frac{1}{2}}+\frac{1}{2}y$
	$\frac{3}{2}, -\frac{1}{2}$	$-1, \frac{1}{2}$	$\frac{1}{6}(1-3x)-\frac{1}{6}[(1-3x)^2+8]^{\frac{1}{2}}-\frac{1}{2}y$
	$\frac{3}{2}, -\frac{3}{2}$	$-1, -\frac{1}{2}$	$-\frac{1}{3}(1+3x)-\frac{3}{2}y$
	$\frac{1}{2}, \frac{1}{2}$	$1, -\frac{1}{2}$	$\frac{1}{6}(1+3x)+\frac{1}{6}[(1+3x)^2+8]^{\frac{1}{2}}+\frac{1}{2}y$
	$\frac{1}{2}, -\frac{1}{2}$	$0, -\frac{1}{2}$	$\frac{1}{6}(1-3x)+\frac{1}{6}[(1-3x)^2+8]^{\frac{1}{2}}-\frac{1}{2}y$
0		1	$x+y$
		0	0
		-1	$-x-y$

2.4 Radio-Frequency Power Required

The rf power required for inducing the high-frequency transitions can be estimated by the approximate requirement that the line width due to power broadening equal the line width caused by the field inhomogeneity. This requirement can be expressed as

$$\frac{1}{h}g_J\mu_0(|J_x|)H_{rf}=\frac{\partial f}{\partial H}\cdot\Delta H,$$

where $(|J_x|)$ is the matrix element of J_x for the transition, f is the frequency of the transition, H_{rf} is the rf magnetic field, and ΔH the field inhomogeneity. When the appropriate numbers are substituted, the above equation becomes

$$\frac{H_{rf}}{\Delta H}\cong\begin{cases}3 \text{ for } D \text{ line}\\ 0.6 \text{ for } E \text{ line}\end{cases}.$$

On the other hand, using appropriate values for the Q and volume of the cavity (see Sec. 5.1) and an appropriate frequency, we find the power required for maintaining a given rf magnetic field in the cavity to be

$$\text{Power in milliwatts}\cong 2000(H_{rf})^2 \quad (H_{rf} \text{ in gauss}).$$

TABLE II. Frequencies of transitions between Zeeman levels of a $^3S_1$ state with $I=\frac{1}{2}$ (He^3) and $I=0$ (He^4) as a function of magnetic field. Frequencies ν are given in units of $\Delta\nu$, the hyperfine splitting at zero field; $x=(g_J-g_I)\mu_0 H/h\Delta\nu$, $y=g_I\mu_0 H/h\Delta\nu$.

I	Name	Transition	$\nu/\Delta\nu$	Approx. field-dep. at low fields, (Mc/sec)/gauss
$\frac{1}{2}$		$(F,m_F)\leftrightarrow(F',m_F')$		
	A_1	$\frac{3}{2}, \frac{3}{2}\leftrightarrow\frac{3}{2}, \frac{1}{2}$	$-\frac{1}{2}(1-x)+\frac{1}{6}[(1+3x)^2+8]^{\frac{1}{2}}+y$	1.9
	A_2	$\frac{3}{2}, \frac{1}{2}\leftrightarrow\frac{3}{2}, -\frac{1}{2}$	$x-\frac{1}{6}[(1+3x)^2+8]^{\frac{1}{2}}+\frac{1}{6}[(1-3x)^2+8]^{\frac{1}{2}}+y$	1.9
	B	$\frac{1}{2}, \frac{1}{2}\leftrightarrow\frac{1}{2}, -\frac{1}{2}$	$x+\frac{1}{6}[(1+3x)^2+8]^{\frac{1}{2}}-\frac{1}{6}[(1-3x)^2+8]^{\frac{1}{2}}+y$	3.7
	D	$\frac{1}{2}, \frac{1}{2}\leftrightarrow\frac{3}{2}, -\frac{1}{2}$	$x+\frac{1}{6}[(1+3x)^2+8]^{\frac{1}{2}}+\frac{1}{6}[(1-3x)^2+8]^{\frac{1}{2}}+y$	2.8
	E	$\frac{1}{2}, -\frac{1}{2}\leftrightarrow\frac{3}{2}, -\frac{3}{2}$	$\frac{1}{2}(1+x)+\frac{1}{6}[(1-3x)^2+8]^{\frac{1}{2}}+y$	0.93
0		$(m_J)\leftrightarrow(m_J')$		
	F_1	$1\leftrightarrow 0$	$x+y$	2.8
	F_2	$-1\leftrightarrow 0$	$x+y$	2.8

[19] I. I. Rabi, Phys. Rev. **51**, 652 (1937).
[20] See R. T. Daly, Jr. and J. R. Zacharias, Phys. Rev. **91**, 476 (1953).
[21] Weinreich, Tucker, and Hughes, Phys. Rev. **87**, 229 (1952).

With $\Delta H=\frac{1}{3}$ gauss, this then means

$$\text{Required power} \cong \begin{cases} 2000 \text{ milliwatts for } D \text{ line} \\ 80 \text{ milliwatts for } E \text{ line} \end{cases}.$$

The Sperry 2K44 klystron used in this experiment, is rated at 250 milliwatts; it is thus seen that, while one can hope to saturate the E line, the D line is bound to be only weakly excited.

2.5 Gas Purity Required[22]

The helium atoms in the discharge tube are excited to the metastable state by collision with electrons and return to the ground state primarily by collision with the walls. In our discharge tube, the average distance from a wall was $\sim$3 mm, and the pressure was such that the mean free path of an atom was $\sim$0.3 mm.

The presence in the discharge tube of impurity atoms adds another mechanism for the quenching of metastables. If we assume that a metastable atom is always quenched by collision with an impurity atom, our criterion for maximum allowable impurity concentration should be that within its mean lifetime a metastable atom does not collide with an impurity atom.

The expected number of collisions with other atoms which a given atom makes in diffusing a distance a is $(a/\lambda)^2$, where λ is the mean free path. Using $a=3$ mm, $\lambda=0.3$ mm, we find $(a/\lambda)^2=100$; and for none of the atoms collided with to be foreign atoms, we must have

$$\text{Maximum impurity fraction} \cong 10^{-2}.$$

The above calculation indicates (in agreement with observed facts) that a few percent of impurity atoms are sufficient to lower the metastable concentration very appreciably.

3. APPARATUS: GAS HANDLING SYSTEM

A total of 3 cc NTP of He^3 was available to us; we designed the gas handling system to work with half of that amount. The system, whose functions can be divided into circulation, storage, and purification, is diagrammed in Fig. 3.

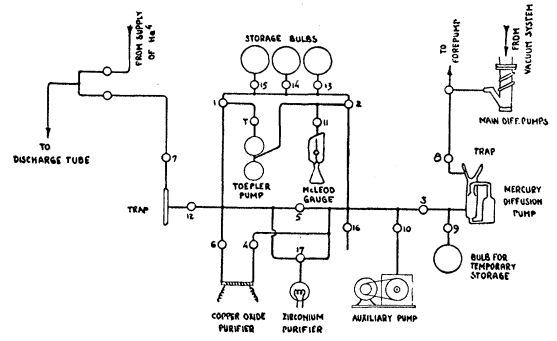

FIG. 3. Gas handling system for helium 3.

[22] See also Appendix I of reference 15.

3.1 Circulation and Storage

Circulation is effected by means of the mercury diffusion pump, which is a type GHG-15 made by Distillation Products, Inc. This pump removes the gas as it comes out of the main diffusion pumps and pumps it back into the discharge tube. The pressure in the return line varies from about 1.5 mm at the output of the mercury pump to a few tenths of a millimeter in the discharge tube. Liquid-nitrogen traps precede and follow the return path.

Alternative connections, labeled "from supply of He^4" and "to forepump" in the figure, were used when no recirculation was required, in particular when a helium-4 beam was run for the purpose of making adjustments on the machine.

Two completely separated storage spaces were available as shown. This was necessary in order to be able to let air into any one part of the system without running into the stored gas. Air had to be admitted for various purposes such as cleaning and greasing stopcocks, changing purifier material, minor glassblowing changes, and admitting and removing the gas.

The Toepler pump had a capacity of 500 cc. The McLeod gauge, with two ranges calibrated from 0.5 micron to 1.8 mm, was connected into the input arm of the Toepler pump.

3.2 Purification by Zirconium

During the planning stage, four substances were considered which would not be trapped on the liquid nitrogen traps and would thus contaminate the gas. These were nitrogen, oxygen, hydrogen, and methane. The first two were expected to present the major problem, since some leakage in the apparatus, notably in the metal system, is unavoidable, and air would thus continually be added to the circulating gas.

Zirconium was chosen as the purifying agent, since at a temperature of about 1300°C it combines with both oxygen and nitrogen, and at about 600°C it adsorbs hydrogen. The purifier was simply a glass bulb with a ground joint and two metal seals supporting a zirconium filament. It could be connected to the system and the impurities allowed to diffuse and combine (see Fig. 3).

It was thought originally that since hydrogen and methane, unlike oxygen and nitrogen, cannot leak into the system, contamination by these gases would present a minor problem at most.

3.3 Purification by Electrodes

The first test of the purification system was made with a sample of helium-4. It was planned to circulate it without purification in order to determine the length of time that it is possible to do so, and then to attempt to purify it. The size of the metastable beam was to be taken as an operational criterion of purity.

The surprising result of this test was that after about five hours of running no decrease in the beam was

observable; in fact, the beam had become somewhat larger. Considering that the idle leak-up rate in the system was of the order of 1 micron/hour and that the volume of the system was about 50 liters, one finds that 10^{-3} mm/hr$\times$50 l$\times$5 hr$=$0.25 mm-l of air should have accumulated during the above run, which amounts to about 20 percent of the total gas. That this amount of contamination (which would have been sufficient to have a strong effect on the color of the discharge, and considerably more than is required to quench the metastable beam) was not, in fact, observed showed that some unplanned but very efficient purifying mechanism was in operation.

This mechanism turned out to be the phenomenon known as "cathode cleanup": the cathode of the discharge tube, which was made of aluminum, was absorbing and/or combining chemically with the impurities. The process was so efficient that, as long as the discharge was on, all the air leakage into the system was continuously and automatically taken care of.

3.4 Purification by Copper Oxide

After twenty or thirty hours of running with He^3, the gas began to show symptoms of severe contamination. First, the metastable beam began to disappear; later the discharge began to take on a pronounced foreign color, and the total amount of gas, as measured by the McLeod gauge, showed a definite increase. Since the original tests with helium-4 indicated that all the impurities introduced in normal operation were removed by the electrodes, it was at first suspected that their cleanup mechanism had for some reason ceased to operate. Changing the cathode, however, produced no improvement.

A spectroscopic observation of the discharge showed the presence of hydrogen. Apparently the cathode was not very efficient in cleaning out this gas, if, indeed, it cleaned it out at all.

The source of this hydrogen, and the reason why it did not show up in the helium-4 trial runs, was not exhaustively investigated; however, two sources can be definitely identified.

(1) Whenever a new cathode was installed, it was first operated with helium-4. During the first five minutes or so the discharge was strongly blue, and the spectrum showed the hydrogen lines as well as a wealth of band structure This was presumably due to organic matter being removed from the cathode surface. With time, the foreign colorations disappeared; if, however, a slow evolution of such matter continued, it would accumulate and show up as contamination after some time.

(2) The other known source of hydrogen was the zirconium purifier. When operating at the high temperatures required for oxygen and nitrogen removal, it dissociated the traces of organic vapors evolved by the vacuum grease.

An electrically heated quartz U-tube of 10-mm o.d. was then filled with CuO and installed in the position shown in Fig. 3 so that, with stopcock No. 5 closed, the gas would pass through it in the course of circulation. The action of the CuO is to oxidize the hydrogen to water (methane to water and carbon dioxide), the product being frozen out on the traps. It was important never to heat the quartz to a high enough temperature to cause devitrification, for it was found that when the quartz became devitrified the purifier would give off hydrogen instead of removing it. At about 550°C, this purifier gave satisfactory service.

4. APPARATUS: DISCHARGE TUBE

In order to be able to work with a minimum amount of gas, it was considered necessary to make all volumes in the system as small as possible. In particular, this applied to the two bulbs around the discharge tube electrodes. The remainder of the discharge tube was the same as that described in reference 15.

The effects of cathode deterioration described below were of special importance in the present experiment because of the limited amount of available gas.

4.1 Anode

Since relatively little heating of the anode occurs in a glow discharge, there was no particular problem in making it reasonably small. It consisted of an aluminum disk $1\frac{1}{2}$ inches in diameter and $\frac{1}{8}$ inch thick, supported by a $\frac{1}{8}$-inch diameter threaded Kovar rod.

4.2 Cathode: Construction

The construction of the water-cooled cathode is shown in Fig. 4. Except for the smaller bulb, it is similar to that used in our previous experiments.

4.3 Cathode: Sputtering

In the experiments on helium-4,[15] the major cathode difficulty was that of sputtering. For a long time (say 30 hr) after a new electrode had been installed, no sputtering was seen. It would then suddenly start at a very rapid rate, so that the change from no visible sputtered film to a film too thick to show interference fringes took place sometimes in the order of minutes.

A few hours after the sputtering had begun, effects detrimental to the operation of the experiment began to appear. The minimum pressure at which a discharge could be maintained rose rapidly. The discharge would go out and, when re-ignited, would glow in quite a different mode, the electrode voltage being about 4000 volts instead of the usual 2500 or so. The power supply was not capable of supplying the customary 100 ma at this voltage, so that the yield of metastables became very low; but even if it had been so capable, the cathode dissipation would probably have been excessive. By

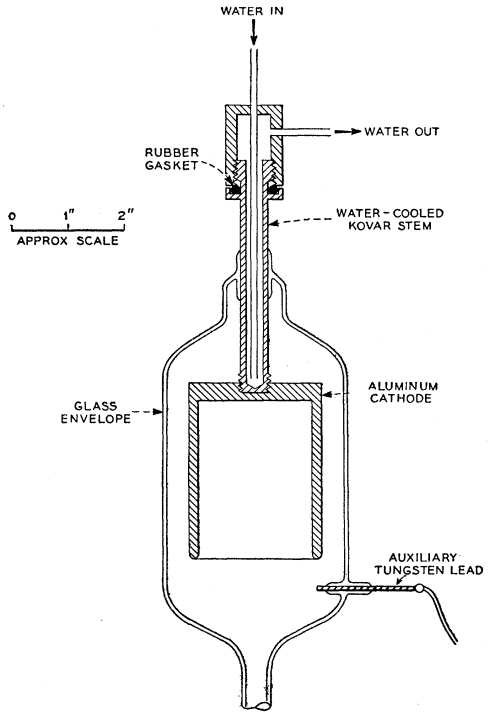

FIG. 4. Construction of cathode. The function of the "auxiliary tungsten lead" is discussed in Sec. 4.3.

increasing the gas pressure in the tube, a discontinuous transition to the usual mode could sometimes be effected; at this point, however, the pressure was so high that an adequate vacuum could not be maintained in the main chamber. In the case of helium-3, the more basic limitation due to the available amount of gas applied.

An explanation of the presence of the high-voltage mode was proposed in terms of the film of sputtered metal acting as a floating electrode. The discharge was thought to break up into two discharges in series, *viz.*, one from cathode to sputtered film, the other from sputtered film to anode. The presence of two cathode falls would qualitatively explain the higher total voltage.

To test this hypothesis, a tungsten lead was sealed into the glass at the point where the sputtered film was expected to appear, with the idea of shorting out one of the two discharges by connecting this lead to the main cathode (Fig. 4). This test gave some support to the two-discharge hypothesis. It was found that when the sputtered film became heavy, connecting the tungsten to the cathode did, in fact, return the discharge to its "normal" mode.

4.4 Cathode: Gas Absorption

The above method of avoiding the ill effects of sputtering did not, however, prove useful, for a more serious problem arose: the "cleanup," or absorption, by the cathode of the helium itself.[23–25] That such a process was taking place was unfortunately not realized in the beginning; thus, about 1 cc NTP of helium-3 was lost.

After the loss had been discovered, frequent checks of gas pressure were made in order to determine how and when the gas was disappearing. It was found that the gas pressure remained constant until the cathode had started to sputter. Some minutes later, the pressure suddenly started to drop at a rate corresponding to the loss of about 0.01 mm-l/min. The discharge was then immediately shut off and the run terminated.

Removing the electrode, scraping off a surface layer, and removing the sputtered film from the glass restored the system to its former nonabsorbing state. In order to prolong the possible running time, two identical electrodes were blown onto the tube. When the first one began to absorb, its electrical lead was disconnected and the second one placed in operation.

It was found that after repeated scrapings the useful life of the cathodes decreased, and the absorption began before any visible sputtering. Finally, a state was reached where scraping did no good at all: the cathode began to absorb as soon as it was placed in operation. Both cathodes were then replaced by new ones; these behaved properly. It thus seems that the absorption process depends on some sort of surface condition which, upon continued exposure, penetrates the body of the material.

There was no obvious relation observed between the purity of the helium and the amount of absorption. On the other hand, no sputtering was ever observed except in fairly pure helium.

5. APPARATUS: RF SYSTEM

5.1 "Hairpin" Design and Construction

The "hairpin," or assembly for impressing rf magnetic fields on the beam, is diagrammed in Fig. 5. It consists of two parts: a rectangular cavity with a fundamental resonant frequency in the vicinity of 7000 Mc/sec, and a loop of copper sheet, $\frac{1}{4}$ in. long along the beam, and terminated in a U-shaped foot near the cavity exit slit. The function of the loop was twofold: it could be used as a source of rf magnetic fields of relatively low frequency (0–1000 Mc/sec); it could also act, due to the placement of the foot, as a monitor of oscillations in the cavity.

The wire stop, also shown in Fig. 5, served to intercept the ultraviolet light from the discharge tube but pass the (deflected) atomic beam. Depending on the placement of the wire, either the $m_J=+1$ or the $m_J=-1$ component could be passed.

Figure 6 shows a cross section, as seen along the

[23] H. Alterthum, Lompe, and Seeliger, Z. tech. Phys. **17**, 407 (1936).
[24] H. Alterthum and A. Lompe, Z. tech. Phys. **19**, 113 (1938).
[25] M. J. Reddan and G. F. Rouse, Trans. Am. Inst. Elec. Engrs. **70**, 1924 (1951).

beam, of the cavity and mounting. The rf was brought in through a coaxial vacuum seal taken from a burned-out Sperry klystron (another such seal was used for connecting to the copper loop). The cavity was attached by six screws to a silver-plated block which contained a tapered coaxial line ending in a small loop which excited the cavity.

Since the gap of the C magnet was $\frac{1}{4}$ in., while the wavelength of the relevant radiation was about seven times that, it was not possible to design a cavity which would have a magnetic field component parallel to the static field. This is the reason why, as mentioned in Sec. 2.2, σ lines were not observable.

As pointed out in Sec. 2.2 (see Fig. 2), the high-frequency resonances observable in the beam, namely the lines D and E, have the frequency $\Delta\nu$ at zero magnetic field and both increase in frequency with an applied magnetic field. In order to be sure of finding the lines, it was therefore necessary to construct the cavity to a frequency high enough so that one could be sure that it was higher than $\Delta\nu$. The previously known optical determination[16] was $\Delta\nu=6630\pm150$ Mc/sec; the cavity was therefore build to have a frequency of 6850 Mc/sec. The inside dimensions of the cavity were 10.0 cm high$\times$2.24 cm long$\times$0.43 cm wide, and it had a Q somewhat greater than 1000.

After a high-frequency line had been observed at this frequency (method 2 of Sec. 6.2 below), it was required to lower the frequency of the cavity to the neighborhood of $\Delta\nu$ (method 3 of Sec. 6.3 below). This was accomplished by placing a strip of Teflon inside the cavity. The strip was of such dimensions as to jam fairly tightly against the sides of the cavity. By moving the Teflon into regions of weaker or stronger rf electric field, one could vary the effective capacitance of the cavity and thus its resonant frequency. It was thus fairly easy to tune it to the required 6740 Mc/sec.

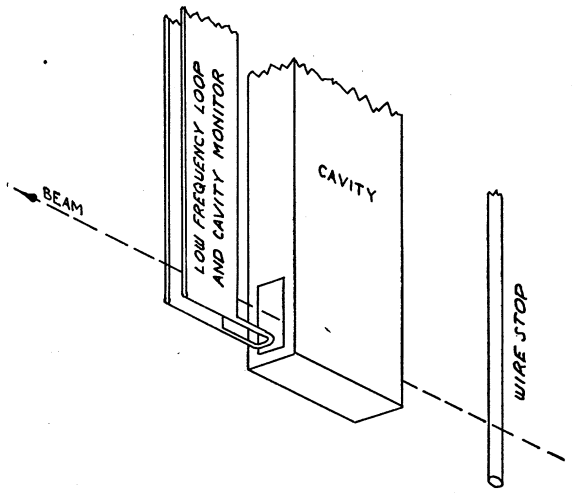

FIG. 5. Arrangement of transition region ("hairpin" assembly).

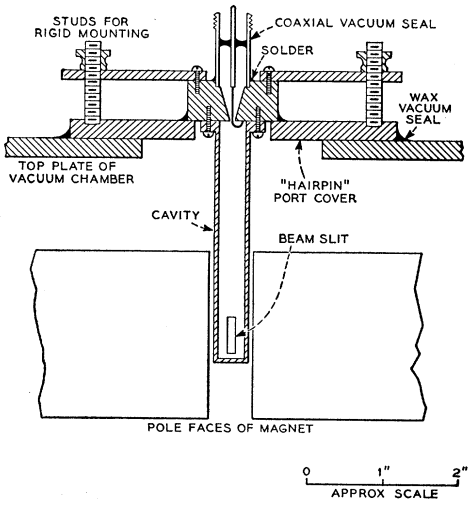

FIG. 6. Construction of cavity and mounting.

The Q of the cavity was not noticeably affected by the introduction of the Teflon.

In tuning the cavity, it was necessary to take into account the change in resonant frequency which occurs upon application of vacuum due to the nonzero dielectric susceptibility of air.

5.2 Radiofrequency Sources

For observing low-frequency resonances, a precision signal generator (General Radio type 805-C) was used up to 50 Mc/sec; a butterfly oscillator (General Radio type 857-A) from 90 to 350 Mc/sec; and a coaxial line lighthouse tube oscillator (radar jammer, APT-5/T-85) from 350 Mc/sec to 1000 Mc/sec.

The source of high-frequency power was a Sperry 2K44 klystron. The klystron was submerged in an oil bath, operated from a regulated power supply, and stabilized against a harmonic of the frequency standard by an automatic frequency control circuit.

5.3 Klystron Automatic Frequency Control

The automatic frequency control circuit was built on the general pattern of that of Lee and Dayhoff.[26] The beat frequency of, say, 50 Mc/sec produced between the klystron and the harmonic of the Columbia frequency standard was fed into an FM receiver (Hallicrafter type S-36). The output of the receiver discriminator was amplified by a dc amplifier and placed on the repeller of the klystron so as to provide negative feedback against frequency changes.

The dc amplifier, of which a circuit diagram is shown in Fig. 7, employed a General Electric 2B23 magnetic amplifier tube, which is a Hull magnetron[27] operating near cutoff. This kind of amplifier has the advantage

[26] C. A. Lee *et al.*, Phys. Rev. **91**, 1403 (1953). E. S. Dayhoff, Rev. Sci. Instr. **22**, 1025 (1951).
[27] A. W. Hull, Phys. Rev. **18**, 31 (1921).

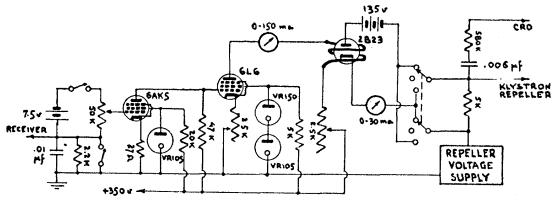

FIG. 7. Dc amplifier for automatic frequency control of 2K44 klystron.

that no dc connection exists between input and output, so that the repeller bias can be changed without adjusting the amplifier.[26]

The brass form for the solenoid which supplied the magnetic field for the 2B23 was slotted to minimize eddy currents and thus improve the frequency response.

Receiver noise presented a problem. Although this noise, as it appeared on the klystron repeller, was cut by a factor of about 20 when the feedback loop was completed, it was still sufficient to increase the band width of the klystron to about 500 kc/sec. It was therefore found necessary to sacrifice frequency response of the amplifier in favor of the decrease in noise obtained by smaller amplifier band width.

An *RC* filter with a time constant of 0.005 sec, placed on the grid of the first dc amplifier stage, cut the noise to a point where the klystron band width was some 15 kc/sec—as good as would be required for this experiment. The price paid for this was that the klystron would jump out of control on a very rapid voltage fluctuation. This was instantly recognizable by a large increase in repeller noise, as seen on a cathode-ray oscilloscope, and by the disappearance of the signal on the receiver *S* meter. Such rapid fluctuations did not occur very often and thus did not present a major problem.

5.4 Measurement of Frequency

Klystron frequencies were measured by tuning in another receiver (National type HRO-50) to the beat of the klystron with another harmonic of the standard. This beat was compared with the output of a crystal-calibrated variable frequency oscillator (General Radio Heterodyne Frequency Meter type 620-A) which was coupled into the same receiver.

It was not possible to use one receiver for both automatic frequency control and frequency measurement, since the signal from the frequency meter would interfere with the automatic frequency control action.

5.5 Cabling and Connections

Figure 8 shows a block diagram of the complete rf system. In order to conserve rf power, the output of the klystron was fed directly into the cavity through a length of RG-9/U cable. The cable from the copper pickup loop came out into a coaxial switch. For observing low-frequency resonances, the switch was connected to the appropriate low-frequency oscillator. For rough tuning of the klystron to the cavity frequency, the switch was connected, through a matching stub, to a crystal and dc meter and the loop thus used as a cavity oscillation monitor. For measurement and automatic frequency control, a third switch position led, again through a matching stub, to a mixer crystal where the signal picked up by the loop was mixed with the frequency standard harmonics. The mixed signal then passed into both receivers through a 100-Mc/sec low-pass filter.

6. METHODS OF MEASURING $\Delta\nu$

At least four methods are available for finding $\Delta\nu$ from measurement of transition frequencies. The first three are progressively more difficult and correspondingly more accurate. The fourth, the most accurate of all, requires an apparatus somewhat different from ours. At some future date, when theoretical advances make it interesting to know a more accurate value for $\Delta\nu$, a modification of the apparatus might be warranted which would make this fourth method possible.

6.1 Method (1): Lines A_1 and F_1

The ratio of the frequencies of transitions A_1 and F_1 (see Table II) at low fields is equal to

$$\tfrac{2}{3}+g_I/3g_J.$$

As the field is increased, however, the frequency A_1 begins to depart from its linear dependence on field, and from the amount of this departure $\Delta\nu$ may be calculated. This method is easy to apply, since one knows at what approximate frequencies to look for these transitions; but it is rather inaccurate, since it depends on the measurement of a small departure from a linear law.

At a field of about 150 gauss, this method was applied, yielding

$$\Delta\nu=6754\pm50 \text{ Mc/sec}.$$

The accuracy here is only three times better than that of the optical measurement;[16] however, this determination served as a general check on the performance of the apparatus and as a valuable guide to later searching.

6.2 Method (2): Lines D and F_1

This method involves the measurement, at a fairly low field, of one of the high-frequency lines in the cavity, and a simultaneous measurement of the F_1 or F_2 line in the low-frequency loop. From the F frequency one calculates the magnetic field, and thus the amount by which the high-frequency line (either the D or the E) has departed from its zero-field value of $\Delta\nu$.

The accuracy here is limited by the fact that the two transitions are not occurring in the same region of the magnet, and the two magnetic field strengths may differ by as much as $\frac{1}{2}$ gauss.[21]

With the cavity tuned to 6850 Mc/sec, a high-frequency line was located by a systematic search. This was identified as the D_2 line by the relative field-dependence of it and the F line. Measurement of both then yielded the result

$$\Delta\nu = 6739 \pm 2 \text{ Mc/sec.}$$

6.3 Method (3): Lines E and D

It can be seen from Fig. 2 that the D and E lines both have the frequency $\Delta\nu$ at zero field. It is not practicable to make atomic beam resonance measurements at zero field because of the loss of space quantization. The Q of the cavity was, however, low enough so that the two lines could be resolved by a small magnetic field ($\sim\frac{2}{3}$ gauss) and still both be within the cavity response, provided that the central frequency of the cavity was correctly adjusted.

In this method, the separation of the lines effectively gives the magnetic-field intensity; after it is known $\Delta\nu$ can be calculated from either frequency. Since both transitions occur in the same region of the magnetic field, the accuracy is limited only by line widths.

This method was the one used in the final measurements.

6.4 Method (4): σ Line

This method, potentially the most accurate one, could not be applied on our apparatus because of the inobservability of σ lines (see Sec. 5.1).

The method depends on the fact that one of the σ lines, *viz.*, the transition $(F, m_F) = (\frac{3}{2}, -\frac{1}{2})$ to $(\frac{1}{2}, -\frac{1}{2})$, has a minimum when the magnetic-field parameter x has a value of $\frac{1}{3}$ (see Fig. 1). This corresponds to a field of about 800 gauss, and the minimum frequency attained by this transition is exactly $\frac{2}{3}\sqrt{2}$ times $\Delta\nu$.

Because of the existence of this minimum, this particular transition is not strongly dependent on the field in this region, and the line width would be determined by the time that an atom spends in the transition region, i.e., the so-called "natural" line width. This width could be very much less than the width observed in our experiment. Since the correction that would need to be applied due to the field not having exactly the intensity necessary for minimum frequency would be of second order, a relatively inaccurate measurement of any other transition would serve to supply this correction.

TABLE III. Summary of data.

Date of observation	D-line, Mc/sec	E-line, Mc/sec	$\Delta\nu$, Mc/sec
February 7, 1953	6741.53	6740.33	6739.73
February 7, 1953	6741.87	6740.42	6739.70
March 7, 1953	6741.50	6740.33	6739.75
March 21, 1953	6741.06	6740.13	6739.67
Mean			6739.71

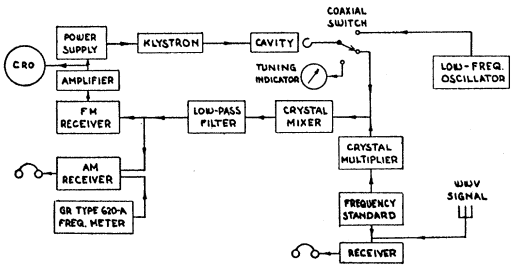

FIG. 8. Block diagram of radiofrequency system.

In order to apply this method, one would need to install a magnet with a gap of 3 or 4 cm and capable of supplying the requisite field.

7. RESULTS

7.1 Line Intensities and Widths

Under good conditions, the E line appeared as a galvanometer deflection of $\sim$7 cm, while the D line was barely more than 1 cm (a 1-cm deflection corresponds to a detector current of about 10^{-15} amp). This relative intensity is in accord with the considerations of Sec. 2.4.

The observed line widths were about $\frac{1}{3}$ Mc/sec for the E line and about 1 Mc/sec for the D line. This, too, agreed with expectations (Sec. 2.3).

7.2 Survey of Data

The result quoted in this paper is an average of four independent measurements (Table III). The range of magnetic fields covered by this data is approximately $\frac{1}{4}$ gauss, as large as could be conveniently encompassed by the response width of the cavity.

The reason why only four runs yielded reliable data, although considerably more than four attempts at obtaining data were made, is primarily the following. At the end of each run, the gas was returned to the storage space by use of the Toepler pump (Sec. 3.1). This operation took about 30 minutes, and any air which leaked into the system during this period was collected together with the helium, since the discharge was off and no purifying action was taking place (Sec. 3.3).

Thus each new run was begun with considerably contaminated helium and no data could be collected before the gas had purified sufficiently. Unfortunately, the time that elapsed during this purification also brought the cathode closer to its "poisoned," or absorbing, condition (Sec. 4.4). In many cases poisoning was reached before sufficient purification or very soon thereafter, and in such a case the run had to be terminated immediately.

7.3 Processing of Data

Three criteria were applied in accepting a given run as significant:

(a) The amplitude of the lines must be large enough so that they can be clearly distinguished from noise.

(b) The ratio of the line widths of the D and E lines must be 3 to 1, as required by theory.

(c) The two lines must be well resolved from one another.

Curves were obtained which represented an average of four to ten traversals of the line in frequency steps which were usually about 100 kc/sec for the (narrow) E line and 300 kc/sec for the (broad) D line; a sample curve, showing both lines, is shown in Fig. 9. The peaks of these curves were determined visually. No significant difference was obtained by three workers performing this determination independently.

7.4 Estimate of Error

The estimate of error quoted here is made on the basis of (a) the probable reliability of determining the peak of a line ($\sim\frac{1}{10}$ of the line width) and (b) the standard deviation of the group of four measurements (0.015 Mc/sec). On this basis, we quote for our final result:

$$\Delta\nu = 6739.71 \pm 0.05 \text{ Mc/sec.}$$

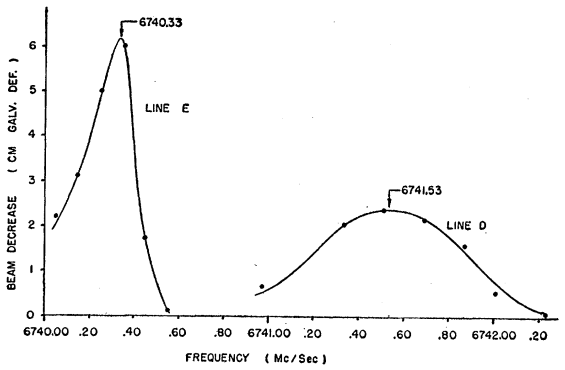

FIG. 9. Data of February 7, 1953, showing the two high-frequency resonances.

7.5 Comparison with Theory

As was pointed out in Sec. 1, the $^3S_1$ wave function for helium is not at present known with sufficient accuracy to make possible a precise calculation of $\Delta\nu$. Nevertheless, it may be of interest to compare our experimental value with such theoretical data as is today available.

Teutsch and Hughes[28] have calculated $\Delta\nu$ for this atomic state using a number of different published electronic wave functions and the value of the He^3 nuclear magnetic moment obtained by Anderson.[29] They have also obtained an estimate of maximum error by comparing the energy eigenvalue give by the particular wave function with the spectroscopically observed energy value.

The most reliable estimate they have obtained is the one from the six-term Hylleraas function. After correcting for reduced mass and for the anomalous electron moment, they obtain

$$\Delta\nu_{\text{theor}} = 6735.9 \pm 4.7 \text{ Mc/sec.}$$

Comparison of this number with the experimental value of the preceding section shows an encouraging agreement; however, the calculation is limited in accuracy by the wave function and necessarily misses all the fine points enumerated in Sec. 1. We are therefore gratified to learn that both Thomas[30] and Luke[31] are at present engaged in calculating a wave function with a precision adequate for a detailed interpretation of our experimental measurement.

8. ACKNOWLEDGMENTS

We wish to thank Professor I. I. Rabi for encouragement and stimulating discussions. Professor T. I. Taylor supplied us with useful advice on purifying methods. Mr. Gerard M. Grosof was of very considerable help in running the apparatus. We are grateful to Mr. Karl Schumann for some masterful glassblowing.

[28] W. B. Teutsch and V. W. Hughes, following paper [Phys. Rev. **94**, 1461 (1954)].
[29] H. L. Anderson, Phys. Rev. **76**, 1460 (1949).
[30] L. H. Thomas (private communication).
[31] P. J. Luke, quoted in reference 14.